DOI: 10.1002/anie.200902543

Metal Aerogels

Hydrogels and Aerogels from Noble Metal Nanoparticles**

*Nadja C. Bigall, Anne-Kristin Herrmann, Maria Vogel, Marcus Rose, Paul Simon, Wilder Carrillo-Cabrera, Dirk Dorfs, Stefan Kaskel, Nikolai Gaponik, and Alexander Eychmüller**

Aerogels are fine inorganic superstructures with enormously high porosity and are known to be exceptional materials with a variety of applications, for example in the area of catalysis.[1] The chemistry of the aerogel synthesis originated from the pioneering work[2] from the early 1930s and was further developed starting from the 1960s.[1,3] Attractive catalytic, thermoresistant, piezoelectric, antiseptic, and many other properties of the aerogels originate from the unique combination of the specific properties of nanomaterials magnified by macroscale self-assembly. Currently, the most investigated materials that form fine aerogel superstructures are silica and other metal oxides together with their mixtures. Recently, the possibility of creating aerogels and even light-emitting monoliths with densities 500 times less than their bulk counterparts from colloidal quantum dots and clusters of metal chalcogenides has attracted attention. These developments may open opportunities in areas such as semiconductor technology, photocatalysis, optoelectronics, and photonics.[4–13]

Quite a number of different approaches have focused on modifying oxide-based aerogels (silica, titania, alumina, etc.) with metal nanoparticles (such as of platinum) to carry the catalytic properties from the metal[14,15] into the porous structures of the aerogels.[1,16,17] Fine mesoporous assemblies of catalytically active metal nanoparticles were also created by using artificial opals[18] and fungi[19] as templates. Other superstructural materials derived from metal nanoparticles include mesoporous platinum–carbon composites,[20] gold nanoparticles interlinked with dithiols,[21] necklace nanochains of hybrid palladium–lipid nanospheres,[22] electrocatalytically active nanoporous platinum aggregates,[23] foams,[24] and highly ordered two- and three-dimensional supercrystals.[25–29]

The creation of non-supported metal aerogels has however not been reported to date. Recently, the formation of highly porous spherical aggregates ("supraspheres") of several hundred nanometers in diameter, where nanoparticles from one or two different metals were cross-linked with dithiols, was reported.[30,31] The metal aerogels presented herein exhibit an average density two orders of magnitude lower than that of the reported foams.[32] Their primary structural units match the size range of single nanoparticles (5–20 nm), which is an order of magnitude smaller than that of the self-assembled supraspheres.[31] Moreover, in the present case, no chemical cross-linkers are involved in the self-assembly process. The formation of such noble-metal nanoparticle-based mesoporous monometallic and bimetallic aerogels is an important step towards self-supported monoliths with enormously high catalytically active surfaces. Considering that metal nanoparticles possess very specific optical properties owing to their pronounced surface plasmon resonance, aerogels from metal nanoparticles may also find future applications in nanophotonics, for example, as advanced optical sensors and ultrasensitive detectors.[33]

In terms of size, shape, and composition control, the synthesis of colloidal metallic nanoparticles is nowadays a well-developed research field.[34–39] For gel formation, various methods of slow destabilization, developed previously for quantum-dot-based gels,[9,13] were systematically applied to aqueous colloidal solutions of gold, silver, and platinum nanoparticles. Supercritical drying[2,40] of the hydrogels with liquid CO_2 finally produces aerogels.

Aqueous colloidal metal solutions are normally very stable in the dilute as-prepared state (below ca. 10^{-8} M particle concentration). To gelate these sols, efficient destabilization is initiated by concentrating the sols (see the Supporting Information). Gel formation is achieved by, for example, the addition of ethanol or hydrogen peroxide to the concentrated colloids.

Different morphologies of the gels can be obtained depending on the type and amount of destabilizer, and also on the metal colloid. Figure 1 shows scanning electron microscopy (SEM; A and B) and transmission electron microscopy (TEM) images (C and D) of an aerogel manufactured from platinum nanoparticles with the use of ethanol as

[*] A.-K. Herrmann, M. Vogel, Dr. N. Gaponik, Prof. Dr. A. Eychmüller
Physical Chemistry/Electrochemistry, TU Dresden
01062 Dresden (Germany)
Fax: (+49) 351-37164
E-mail: Alexander.eychmueller@chemie.tu-dresden.de
Homepage: http://www.chm.tu-dresden.de/pc2/index.shtml
Dr. N. C. Bigall, Dr. D. Dorfs
Istituto Italiano di Tecnologia
via Morego 30, 16163 Genova (Italy)
M. Rose, Prof. Dr. S. Kaskel
Inorganic Chemistry, TU Dresden
01062 Dresden (Germany)
Dr. P. Simon, Dr. W. Carrillo-Cabrera
Max-Planck-Institut für Chemische Physik fester Stoffe
01187 Dresden (Germany)

[**] We thank the European NoE PHOREMOST and DFG Project EY16/10-1 for financial support, Ellen Kern for performing scanning electron micrographs, and Prof. Lichte for use of the High-Resolution Electron Microscopy and Electron Holography Laboratory Triebenberg at the TU Dresden (Germany).

Supporting information for this article (including methods, a detailed description of the experimental results, and further characterization) is available on the WWW under http://dx.doi.org/10.1002/anie.200902543.

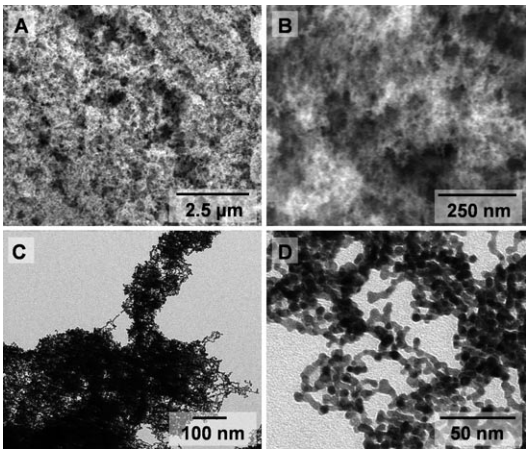

Figure 1. A, B) SEM and C, D) TEM images of aerogels from platinum nanoparticles destabilized from solution by the addition of ethanol. The fractal morphology of the gel is homogeneously dispersed over large areas of the sample. The gel consists of nanoparticles of approximately the same size as those in the original sol.

destabilizer. The aerogel that is obtained is composed of ultrathin structures that have typical dimensions on the same size scale as the diameter of the original nanoparticles (4–5 nm). Therefore, the aerogel seems to be formed directly from the original colloidal particles without previous agglomeration into any kind of secondary structures.

In the case of gold, the addition of H_2O_2 results in the formation of gels from secondary or tertiary particles (Supporting Information, Figure S5). Moreover, the morphology can be controlled by the amount of H_2O_2 added. However, the grain size obtained (hundreds of nanometers) is much larger than the size of the original gold nanoparticles (3–6 nm).

Another example is given by silver nanoparticles destabilized by hydrogen peroxide (Supporting Information, Figure S6). The resulting aerogel is composed of grains with a diameter of around 50 nm, thus again consisting of some sort of pre-agglomerated secondary particles and not of the original colloidal particles.

Although these attempts of forming monometallic aerogels from gold, silver, and platinum have been successful, we observed variations in the reproducibility. The reasons may be differences in the concentrations of the components in the colloidal solutions and slight deviations in the environmental conditions during the relatively long time (weeks to months) required for gel formation.

Clear differences between mono- and bimetallic gel formations can be observed in their effective destabilization agents and timescales of formation, and also in their microscopic properties. From mixtures of concentrated gold and silver nanoparticle solutions we were able to form gels with strongly increased reproducibility, whilst decreasing the duration of the process, obtaining more voluminous gels, and preventing morphologies with grains of higher orders. The addition of a small amount of 30% hydrogen peroxide or of pure ethanol caused the formation of black and very voluminous macroscopic gels after about ten days. Moreover, without the addition of any destabilizing agents, the formation of a voluminous gel is observed approximately 15 days after mixing the concentrated gold and silver nanoparticle solutions.

All the gels obtained by mixing gold and silver nanoparticles had no characteristic color, but instead were black. Figure 4A is a color photograph of a gold/silver hydrogel. Shortly after gel formation, we were able to observe a slightly colored supernatant solution. After a few days, the supernatant solution was completely colorless, thus confirming that all nanoparticles were associated with the gel.

As can be seen from the TEM image in Figure 2A, the structure has a wire-like morphology with typical thicknesses of between 3 and 10 nm and several branch points. Unlike other gels from nanoparticles,[10] the present morphology does not show single nanoparticles well-separated from each other, but rather a fused wire-like structure. High-resolution TEM analysis of selected areas (Figure 2B and C) reveals the

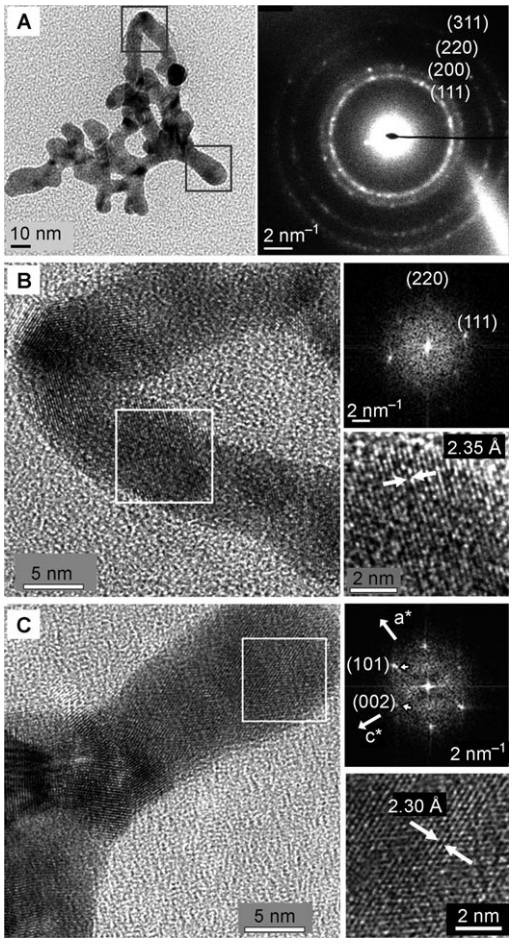

Figure 2. A) Left: TEM overview image of a gold/silver hydrogel after drying from methanol onto a TEM grid. Right: Electron diffraction showing typical lattice planes of gold or silver. B) Left: HR-TEM image of the area taken from (A, left), showing a kink of 60°. Right: One of the condensed dots marked with the white frame in the center is displayed enlarged on the right with the corresponding FFT ([112] zone). C) Left: "Nanofinger" ($\varnothing \approx 12$ nm) corresponding to the zoomed area from (A, left). The HR image (C, bottom right) and the corresponding FFT image (C, top right), [010] zone, indicate the presence of hexagonal silver. This sample was obtained without addition of destabilizer.

polycrystallinity of the network formed. The electron diffraction micrograph of the hydrogels show typical spacings of fcc gold or silver crystals of 2.37 Å (111), 2.05 Å (200), 1.47 Å (220) and 1.23 Å (311) (Figure 2A, right). The crystallographic parameters of fcc gold and silver are very similar so that the two materials are crystallographically non-distinguishable. The gel is highly cross-linked, and consists of bent nanowires with diameters of 7–11 nm. The magnified area taken from the frame in the top (Figure 2A, left) shows a sharp bend with an opening angle of about 60°. The nanowires are composed of laterally fused single-crystalline nanoparticles of different sizes. These subunits (nanodots) are single crystals. In Figure 2B (right), one nanodot is shown enlarged with the corresponding fast Fourier transform (FFT) of the [112] zone of regular cubic silver or gold.

Some wires give rise to free ends, such as the "nanofinger" shown in Figure 2C. The FFT and the corresponding HR-TEM image (Figure 2C, right) indicate the [010] zone of a single-crystal silver nanoparticle with hexagonal crystal symmetry similar to that described by Novgorodova et al;[41] to date, a hcp modification of gold is not known. Lattice spacings indicate an elongated *a* axis (3.00 Å instead of 2.93 Å) and also an elongated *c* axis (4.94 Å instead of 4.79 Å). This difference from more accurate values, such as X-ray diffraction data, is within the experimental calibration error of the TEM. With these settings, the distance of 2.30 Å can be labeled as (101) and 2.47 Å as (002). Nevertheless, the observed spacings are too small to be ascribed to any variant of silver oxide or silver hydroxide. The regular cubic lattice is observed throughout the wire region and is ascribed to a gold-rich alloy, whereas the ends (the finger structures) within the aggregates are attributed to a hexagonal silver-rich alloy.

The gel formation processes are reproducible under analogous conditions. The time needed for gel formation may vary by a few days from nanoparticle batch to nanoparticle batch, but within one batch, this time remains constant.

The hydrogels can be dried supercritically whilst the macroscopic sizes of the gels are retained. Scanning electron micrographs (SEMs) of a resulting aerogel are shown in Figure 3. The fine wire-like structures with many bifurcations and thicknesses of a few nanometers can also be clearly seen in this case. Energy-dispersive X-ray (EDX) mapping reveals equal distributions of gold and silver over the entire structure (Figure 4C). The atomic ratio of gold to silver is close to one (0.43:0.57). Photographs of a piece of the black gold/silver hydrogel and aerogel are depicted in Figure 4A and 4B, respectively. The aerogel shown has a diameter of around 3–4 mm, and the average density of the material is 0.016 $g\,cm^{-3}$, which corresponds to approximately one thousandth of the averaged bulk density of gold and silver, thus showing the unique physical properties of this new type of material.

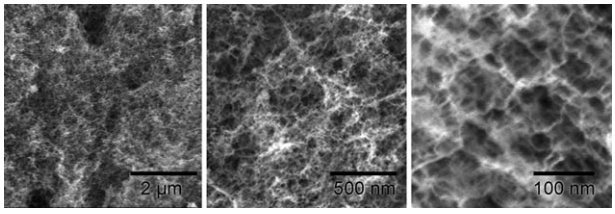

Figure 3. SEM images of a bimetallic gold/silver aerogel at different magnifications. This sample was destabilized from solution by the addition of H_2O_2.

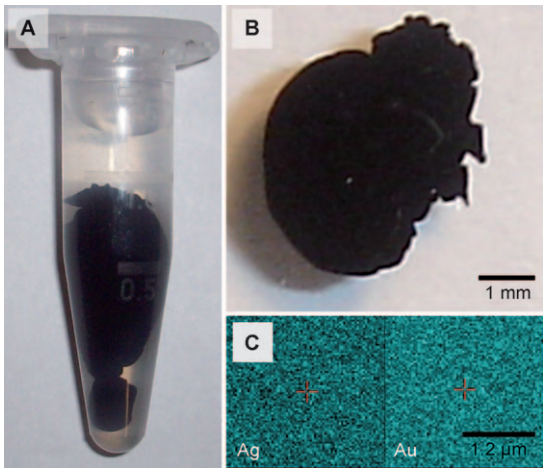

Figure 4. a) Photograph of a gold/silver hydrogel, and B) of a piece of the corresponding aerogel. C) EDX mapping of the aerogel, showing equal distributions of gold and silver. This sample was destabilized from solution by the addition of H_2O_2.

Similarly, bimetallic aerogels can be produced from mixtures of colloidal silver and platinum nanoparticles. In this case as well, no additional destabilizer is needed, because hydrogels are formed readily in the colloidal mixture after 15 days without the addition of any destabilizing agent. These dried aerogels show a morphology that seems to suggest that the gels are composed of the as-synthesized nanocrystals without further alloying or growth of secondary particles (see SEM and TEM images in Figure 5).

As the unit cell parameters of platinum are significantly smaller than those of silver, we expect to be able to distinguish between these two elements by HR-TEM for particles in the same image. For example, the (111) lattice spacing is 2.26 Å for platinum and 2.36 Å for silver.[42] As shown in Figure 5E, two of the particles have been identified as platinum and two as silver nanocrystals.

Furthermore, the distribution of silver and platinum within a small piece of a dried hydrogel was investigated by EDX elemental mapping (see the Supporting Information). Although there are slight lateral variations in the presence of the elements, to a large extent the images yield evidence of a homogeneous platinum and silver distribution.

Nitrogen adsorption measurements (BET method) on the silver/gold and platinum/silver aerogels after activation at 50 °C revealed very large surface areas of 48 $m^2 g^{-1}$ (Ag/Au) per gram and 46 $m^2 g^{-1}$ (Pt/Ag), which is consistent with the surface of 38 m^2 per gram obtained by estimation under the assumption of a long network of wires with 7 nm diameter and average density of 15 $g\,cm^{-3}$. In the case of the silver/gold aerogel, this result corresponds to a molar surface of 7.2×10^3 $m^2\,mol^{-1}$. For comparison, typical silica aerogels have molar surfaces of 30×10^3 and maximum values of approximately 10×10^4 $m^2\,mol^{-1}$. The metal aerogel surface could be acting entirely as an active area in an application such as

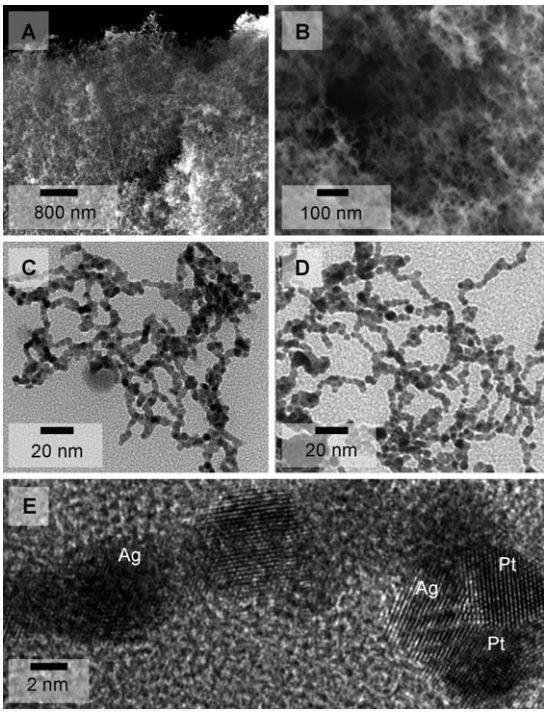

Figure 5. A,B) SEM images of platinum/silver aerogels at different magnifications, and C,D) TEM micrographs of a platinum/silver hydrogel (C) and aerogel (D). E) HR-TEM image of the platinum/silver nanochains, showing individual silver and platinum nanodots (diameters of ca. 3–6 nm). The lattice distances for the particles indicated were $d(111)_{Ag} = 2.36$ Å and $d(111)_{Pt} = 2.22$ Å. This sample was obtained without addition of destabilizer.

catalysis, as these structures do not contain any carrier substrate, but consist nearly completely of the catalytically active materials, such as silver, gold, or platinum. The direct contact between nanoparticles forming the percolating aerogel structure is responsible for the observed conductivity of bulk aerogel species. The resistance found for a piece of gold/silver aerogel that is 2–3 mm in diameter is in the range of 10–100 kΩ.

Although the underlying mechanism of gel formation is still to be determined, we consider silver to play the role of a linking metal, because we have not yet been able to produce bimetallic aerogels from gold and platinum sol.

Received: May 13, 2009
Revised: August 10, 2009
Published online: November 13, 2009

Keywords: aerogels · bimetallic nanostructures · hydrogels · metal nanoparticles

[1] N. Hüsing, U. Schubert, *Angew. Chem.* **1998**, *110*, 22; *Angew. Chem. Int. Ed.* **1998**, *37*, 22.
[2] S. S. Kistler, *Nature* **1931**, *127*, 741.
[3] H. D. Gesser, P. C. Goswami, *Chem. Rev.* **1989**, *89*, 765.
[4] S. L. Brock, I. U. Arachchige, K. K. Kalebaila, *Comments Inorg. Chem.* **2006**, *27*, 103.
[5] S. Bag, I. U. Arachchige, M. G. Kanatzidis, *J. Mater. Chem.* **2008**, *18*, 3628.
[6] S. Bag, P. N. Trikalitis, P. J. Chupas, G. S. Armatas, M. G. Kanatzidis, *Science* **2007**, *317*, 490.
[7] S. Bag, M. G. Kanatzidis, *J. Am. Chem. Soc.* **2008**, *130*, 8366.
[8] J. L. Mohanan, I. U. Arachchige, S. L. Brock, *Science* **2005**, *307*, 397.
[9] I. U. Arachchige, S. L. Brock, *Acc. Chem. Res.* **2007**, *40*, 801.
[10] I. U. Arachchige, S. L. Brock, *J. Am. Chem. Soc.* **2006**, *128*, 7964.
[11] A. Eychmüller, *Angew. Chem.* **2005**, *117*, 4917; *Angew. Chem. Int. Ed.* **2005**, *44*, 4839.
[12] I. U. Arachchige, S. L. Brock, *J. Am. Chem. Soc.* **2007**, *129*, 1840.
[13] N. Gaponik, A. Wolf, R. Marx, V. Lesnyak, K. Schilling, A. Eychmüller, *Adv. Mater.* **2008**, *20*, 4257.
[14] C. T. Campbell, *Science* **2004**, *306*, 234.
[15] Y. Jiang, Q. Gao, *J. Am. Chem. Soc.* **2006**, *128*, 716.
[16] G. M. Pajonk, *Catal. Today* **1997**, *35*, 319.
[17] A. Vallribera, E. Molins, *Nanopart. Catal.* **2008**, 161.
[18] L. Lu, R. Capek, A. Kornowski, N. Gaponik, A. Eychmüller, *Angew. Chem.* **2005**, *117*, 6151; *Angew. Chem. Int. Ed.* **2005**, *44*, 5997.
[19] N. C. Bigall, M. Reitzig, W. Naumann, P. Simon, K.-H. van Pee, A. Eychmüller, *Angew. Chem.* **2008**, *120*, 7994; *Angew. Chem. Int. Ed.* **2008**, *47*, 7876.
[20] S. C. Warren, L. C. Messina, L. S. Slaughter, M. Kamperman, Q. Zhou, S. M. Gruner, F. J. DiSalvo, U. Wiesner, *Science* **2008**, *320*, 1748.
[21] Y. Joseph, B. Guse, G. Nelles, *Chem. Mater.* **2009**, *21*, 1670.
[22] Y. Zhou, M. Kogiso, T. Shimizu, *J. Am. Chem. Soc.* **2009**, *131*, 2456.
[23] B. Viswanath, S. Patra, N. Munichandraiah, N. Ravishankar, *Langmuir* **2009**, *25*, 3115.
[24] J. Banhart, *Prog. Mater. Sci.* **2001**, *46*, 559.
[25] A. M. Kalsin, M. Fialkowski, M. Paszewski, S. K. Smoukov, K. J. M. Bishop, B. A. Grzybowski, *Science* **2006**, *312*, 420.
[26] E. V. Shevchenko, D. V. Talapin, N. A. Kotov, S. O'Brien, C. B. Murray, *Nature* **2006**, *439*, 55.
[27] C. J. Kiely, J. Fink, M. Brust, D. Bethell, D. J. Schiffrin, *Nature* **1998**, *396*, 444.
[28] E. Rabani, D. R. Reichman, P. L. Geissler, L. E. Brus, *Nature* **2003**, *426*, 271.
[29] H. Fan, K. Yang, D. M. Boye, T. Sigmon, K. J. Malloy, H. Xu, G. P. Lopez, C. J. Brinker, *Science* **2004**, *304*, 567.
[30] R. Klajn, K. J. M. Bishop, M. Fialkowski, M. Paszewski, C. J. Campbell, T. P. Gray, B. A. Grzybowski, *Science* **2007**, *316*, 261.
[31] R. Klajn, T. P. Gray, P. J. Wesson, B. D. Myers, V. P. Dravid, S. K. Smoukov, B. A. Grzybowski, *Adv. Funct. Mater.* **2008**, *18*, 2763.
[32] J. Schroers, C. Veazey, W. L. Johnson, *Appl. Phys. Lett.* **2003**, *82*, 370.
[33] Y. W. C. Cao, R. Jin, C. A. Mirkin, *Science* **2002**, *297*, 1536.
[34] Y. Sun, Y. Xia, *Science* **2002**, *298*, 2176.
[35] K. R. Brown, D. G. Walter, M. J. Natan, *Chem. Mater.* **2000**, *12*, 306.
[36] G. Frens, *Nature Phys. Sci.* **1973**, *241*, 20.
[37] J. Turkevich, P. C. Stevenson, J. Hillier, *Discuss. Faraday Soc.* **1951**, *11*, 55.
[38] T. S. Ahmadi, Z. L. Wang, T. C. Green, A. Henglein, M. A. El-Sayed, *Science* **1996**, *272*, 1924.
[39] N. C. Bigall, T. Härtling, M. Klose, P. Simon, L. M. Eng, A. Eychmüller, *Nano Lett.* **2008**, *8*, 4588.
[40] P. H. Tewari, A. J. Hunt, K. D. Lofftus, *Mater. Lett.* **1985**, *3*, 363.
[41] M. I. Novgorodova, A. I. Gorshkov, A. V. Mokhov, *Zap. Vses. Mineral. O-va.* **1979**, *108*, 552.
[42] H. E. Swanson, E. Tatge, *Natl. Bur. Stand. Circ.* **1953**, *539*, 95.

